# A superconducting 180° hybrid ring coupler for circuit quantum electrodynamics

E. Hoffmann,[1,2,a)] F. Deppe,[1,2] T. Niemczyk,[1,2] T. Wirth,[3] E. P. Menzel,[1,2] G. Wild,[1,2] H. Huebl,[1,2] M. Mariantoni,[1,2] T. Weißl,[1,2] A. Lukashenko,[3] A. P. Zhuravel,[4] A. V. Ustinov,[3] A. Marx,[1] and R. Gross[1,2,b)]

[1]*Walther-Meißner-Institut, Bayerische Akademie der Wissenschaften, 85748 Garching, Germany*
[2]*Physik-Department, Technische Universität München, 85748 Garching, Germany*
[3]*Karlsruher Institut für Technologie (KIT), Physikalisches Institut, 76128 Karlsruhe, Germany*
[4]*B. I. Verkin Institute for Low Temperature Physics and Engineering, National Academy of Sciences of Ukraine, 61103 Kharkov, Ukraine*

(Received 10 June 2010; accepted 9 November 2010; published online 3 December 2010)

Superconducting circuit quantum electrodynamics experiments with propagating microwaves require devices acting as beam splitters. Using niobium thin films on silicon and sapphire substrates, we fabricated superconducting 180° microstrip hybrid ring couplers, acting as beam splitters with center frequencies of about 6 GHz. For the magnitude of the coupling and isolation, we find $-3.5\pm0.5$ dB and at least $-15$ dB, respectively, in a bandwidth of 2 GHz. We also investigate the effect of reflections at the superconductor-normal conductor contact by means of low temperature laser scanning microscopy. Our measurements show that our hybrid rings are well suited for on-chip applications in circuit quantum electrodynamics experiments. 
[doi:10.1063/1.3522650]

In superconducting circuit quantum electrodynamics (QED),[1–3] intracavity microwave photons interact with solid-state artificial atoms.[4–6] Both cavity and atom are realized by superconducting quantum circuits on a chip with characteristic frequencies in the microwave regime (1–10 GHz). Recently, this field has been extended toward the study of propagating quantum microwaves. To this end, quantum optical techniques, such as optical homodyne tomography[7] or photon-based quantum information processing and communication,[8,9] are being adapted to the microwave regime. One key element for the transformation from the optical to the microwave regime is the implementation of a beam splitter, which is understood on the quantum level.[10] This allows to use signal recovery techniques, employing two amplifier chains and eliminating the (not yet available) single microwave photon detectors.[11] Hereby, photon correlations can be accessed and all quadrature moments of propagating quantum microwaves and, simultaneously, those of the detector noise can be extracted.[12] The very same idea was recently used to characterize the blackbody radiation emitted by a 50 Ω load resistor.[13] Ideally, in experiments with propagating quantum microwaves, a beam splitter has to be lossless. A device that matches these conditions is the 180° hybrid ring, which is entirely based on interference effects. Usually, microwave beam splitters are realized as normal conductive devices. However, for superconducting circuit QED, the on-chip implementation of the beam splitter and the superconducting quantum devices under investigation would be favorable, avoiding reflections between various circuit parts and minimizing interconnect losses.

In this letter, we present a detailed study on low-loss superconducting hybrid rings fabricated from niobium microstrip lines on both silicon and sapphire substrates. For the magnitude of the coupling and isolation, we find $-3.5\pm0.5$ dB and better than $-15$ dB in a bandwidth of up to 2 GHz, respectively. We note that the isolation increases when reducing the bandwidth, reaching a maximum value of better than $-60$ dB at the center frequency. Our measurements indicate that the device performance is limited by reflections between the superconducting parts on the chip and the normal conducting microwave connectors. This conclusion is based on our data obtained by low temperature laser scanning microscopy (LTLSM).[14,15] Our experiments indicate that our hybrid ring couplers are highly suitable for integration into superconducting circuit QED experiments,[16] ultimately allowing for studies of propagating quantum microwaves[11–13] and applications in quantum information processing.

The 180° hybrid ring is sketched in Fig. 1(a). It consists of a superconducting ring with four signal ports. The circumference $U=1.5\lambda$ of the ring determines the center frequency $f_0=v_{ph}/\lambda$ of the device. Here, $v_{ph}$ is the phase velocity of electromagnetic waves and $\lambda$ is the wavelength. An input signal of frequency $f$ incident at port 1 (or 3) is split into its clockwise and counterclockwise propagating components, which interfere constructively (3 dB coupling) at ports 2 and

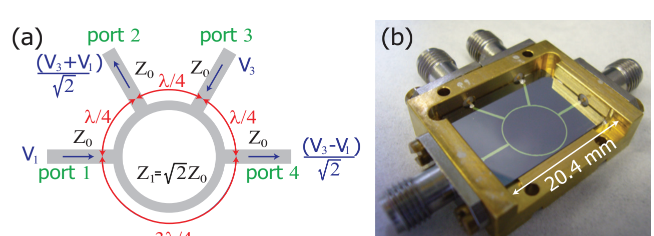


FIG. 1. (Color) (a) Schematic of a 180° hybrid ring. In this configuration, ports 1 and 3 act as input ports, while ports 2 and 4 are output ports. (b) Photograph of a niobium hybrid ring fabricated on a silicon substrate and mounted inside a gold-plated copper box.

a)Electronic mail: elisabeth.hoffmann@wmi.badw-muenchen.de.
b)Electronic mail: rudolf.gross@wmi.badw-muenchen.de.

 

4, whereas they interfere destructively (isolation) at ports 3 and 1. When two signals are applied to ports 1 and 3, their sum and difference is present at ports 2 and 4, respectively. To avoid reflections and to guarantee an equal splitting of the signal, the impedance of the ring[17,18] must be chosen as $Z_1 = Z_0\sqrt{2} = 71\ \Omega$ for a feed line impedance $Z_0 = 50\ \Omega$.

The hybrid rings are based on 200 nm thick niobium films deposited by magnetron sputtering and patterned by optical lithography and reactive ion etching using $SF_6$. Niobium is chosen due to its high critical temperature of 9.2 K. As substrate materials we use silicon (thickness of 525 $\mu$m and dielectric constant $\varepsilon_r = 11.9$) covered by 50 nm of silicon dioxide, as well as sapphire (thickness of 500 $\mu$m and $\varepsilon_r = 10.2$). Although recent measurements at millikelvin temperatures[19] show loss tangents of $\simeq 10^{-5}$ for both crystalline materials sapphire and silicon, we need to verify to what extent the amorphous $SiO_2$ coating of our silicon substrates affects the device performance. The radius of all studied hybrid rings is 4.78 mm, corresponding to $f_0 = 5.6$ GHz (6 GHz) for the samples on silicon (sapphire). The microstrip lines forming the input and output ports are 420 $\mu$m (490 $\mu$m) wide for the devices on silicon (sapphire). The width of the strip forming the ring is 171 $\mu$m (221 $\mu$m). For the characterization of the microwave properties, the chip is mounted inside a gold-plated copper box, as shown in Fig. 1(b), and then cooled down in a $^4$He cryostat. We recorded the coupling and isolation properties of seven (four) different hybrid rings fabricated on silicon (sapphire) substrates. Each chip is remounted, cooled down, and remeasured several times to test the reproducibility.

The performance of the hybrid rings is studied by measuring the scattering matrix $S_{ij}$ $(i,j = 1,\ldots,4)$ using a two-port vector network analyzer. We only measured the scattering parameters with $i \neq j$ by connecting ports $i$ and $j$ to the network analyzer, while the other two ports are terminated right at the sample box with 50 $\Omega$ loads. The characteristics of our hybrid rings fabricated on sapphire and silicon substrates are shown in Figs. 2(a)–2(d). Figures 2(a) and 2(c) display the $S$-parameters for constructive interference at the respective output port. For both substrate materials, we find a coupling magnitude of $-3.3 \pm 0.2$ dB at the center frequency $f_0$, as expected for a $-3$ dB beam splitter. Within a bandwidth of 2 GHz around $f_0$, the coupling magnitude is in the range of $-3.5 \pm 0.5$ dB. Well outside this frequency window, it drops below $-10$ dB, reflecting the considerable mismatch between the device circumference $U$ and $1.5\lambda$ at the test frequency. The isolation of the devices is shown in Figs. 2(b) and 2(d) for sapphire and silicon substrates, respectively. In both cases, the isolation magnitude exceeds $-15$ dB within the full bandwidth of 2 GHz around $f_0$, showing the excellent performance of the hybrid rings. We note that despite the $SiO_2$ coating of the silicon substrate, the performance of our hybrid rings is robust with respect to dielectric losses.

In some of our devices, we find characteristic changes in the transmission data when remounting and remeasuring the same device. First, the frequency of the maximum isolation may shift and a "hump" may appear in the spectrum, as shown in Fig. 2(d). Concurrently, the coupling spectra may become asymmetric and their magnitudes at the center frequency may vary slightly, as indicated in Fig. 2(c). The likely origin of these features are reflections at the contact between the superconducting on-chip feed lines and the normal conducting microwave connectors, which affect the interference pattern in the ring. To explore these artifacts, we visualize the effects of reflections by measuring the response of a hybrid ring on a silicon substrate to local heating by a focused laser beam. This method is known as low temperature laser scanning microscopy.[14] In these experiments, a focused laser beam is scanned across the chip surface and the change in the transmission parameter $S_{42}$ is recorded as a function of the beam position. Local heating by the focused laser beam results in quasiparticle generation in the niobium film.[20] Therefore, local Ohmic dissipation proportional to the high frequency electrical field changes the transmission magnitude.

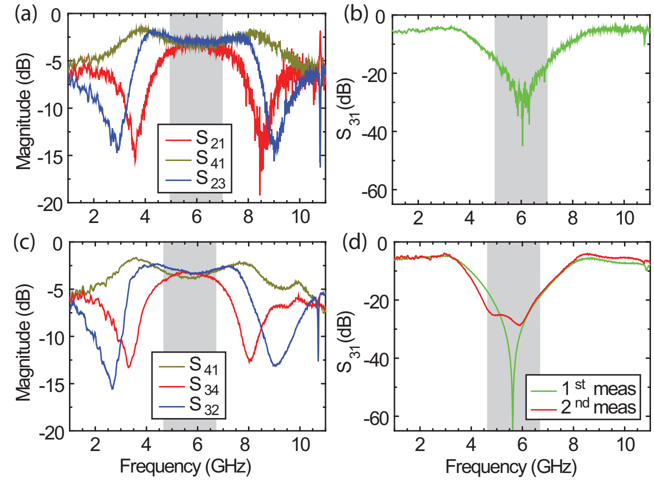


FIG. 2. (Color) Typical transmission data for hybrid rings on sapphire [panels (a) and (b)] and silicon [panels (c) and (d)] substrates measured at 4.2 K with an input power of $-40$ dBm. For both materials, we observe a coupling of $-3.5 \pm 0.5$ dB and an isolation of at least $-15$ dB within a bandwidth of 2 GHz (gray background) around the center frequency. Note that the different noise levels are not related to the substrate material but are caused by the difference in the measurement protocol: no averaging in (a) and (b); 20 times averaging in (c) and (d). Additionally, in (d) $S_{31}$ is shown for the same sample after remounting it. While the green curve shows a close-to-ideal spectrum, the red curve shows a hump caused by reflections at the chip-connector contact (cf. Fig. 3). In the coupling spectra of (c), such reflections manifest themselves as an asymmetry. In all measurements, a box resonance at approximate 11 GHz can be seen.

The LTSLM images shown in Figs. 3(c) and 3(d) can be understood in a straightforward way. With an input signal at the center frequency $f_0$ at port 2, the interference in the ring is expected to lead to three maxima, two of them located at ports 1 and 3, and three minima, two of them are expected to be found at ports 2 and 4, as depicted in Fig. 3(a). The transmission $S_{42}$ without laser irradiation measured with a vector network analyzer in the LTLSM setup is plotted in Fig. 3(b), showing the combination of a hump and a shifted minimum at 4.93 GHz. In Fig. 3(c), the spatially resolved transmission magnitude at the hump frequency is displayed. First, we notice maxima in the feed lines (marked green), which indicate standing waves caused by reflections at the connectors. Second, although the electric field maxima and minima on the ring are slightly shifted from their ideal positions, they are still located near the expected ports. Consequently, there remains significant isolation between ports 2 and 4. Third, when changing the excitation frequency to the isolation maximum at 4.93 GHz, the ideal interference pattern is restored in the ring, as shown in Fig. 3(d). Neverthe-

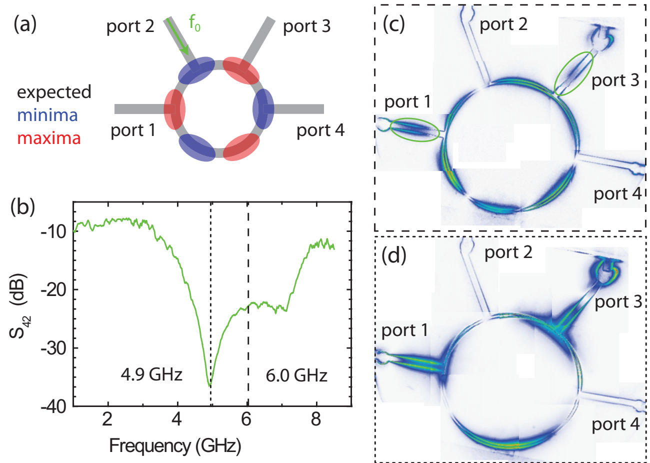


FIG. 3. (Color) (a) Expected spatially resolved transmission magnitude at the center frequency $f_0$ where the isolation should reach its minimum. Port 2 is used as input port. (b) Measurement of the integral $S_{42}$ isolation at 4.2 K with a network vector analyzer attached to the LTLSM apparatus. (c) LTLSM data taken at the hump (6 GHz; color code: transmission magnitude). (d) LTLSM data taken at 4.93 GHz, where the isolation is maximal.

less, there is still a significant signal in the feed lines due to the reflections from the connectors.

In conclusion, we have fabricated superconducting 180° hybrid ring couplers on both sapphire and silicon substrates. Within a 2 GHz bandwidth around the center frequency of around 6 GHz, the devices show an almost ideal coupling of $-3.5\pm0.5$ dB. Furthermore, we find an isolation of at least $-15$ dB. The observed imperfections are clearly attributed to the remaining reflections at the transition between the superconducting on-chip feed lines and the normal conducting microwave connectors, demonstrating the importance of proper mounting. The performance of our hybrid rings is suitable for further experiments with propagating quantum microwaves, e.g., in the spirit of those presented in Ref. 12 or Ref. 13.

We thank A. Emmert for useful discussions. For financial support, we acknowledge the Deutsche Forschungsgemeinschaft via SFB 631 and CFN, EU project SOLID, and the German Excellence Initiative via NIM.

[1]A. Wallraff, D. Schuster, A. Blais, L. Frunzio, R.-S. Huang, J. Majer, S. Kumar, S. Girvin, and R. Schoelkopf, Nature (London) **431**, 162 (2004).
[2]A. Blais, R.-S. Huang, A. Wallraff, S. M. Girvin, and R. J. Schoelkopf, Phys. Rev. A **69**, 062320 (2004).
[3]I. Chiorescu, P. Bertet, K. Semba, Y. Nakamura, C. Harmans, and J. Mooij, Nature (London) **431**, 159 (2004).
[4]Y. Makhlin, G. Schön, and A. Shnirman, Rev. Mod. Phys. **73**, 357 (2001).
[5]M. Devoret, A. Wallraff, and J. Martinis, e-print arXiv:cond-mat/0411174.
[6]J. Clarke and F. K. Wilhelm, Nature (London) **453**, 1031 (2008).
[7]U. Leonhardt, *Measuring the Quantum State of Light* (Cambridge University Press, Cambridge, 1997).
[8]D. Bouwmeester, A. Ekert, and A. Zeilinger, *The Physics of Quantum Information* (Springer, Berlin, 2000).
[9]J. L. O'Brien, Science **318**, 1567 (2007).
[10]M. Mariantoni, M. J. Storcz, F. K. Wilhelm, W. D. Oliver, A. Emmert, A. Marx, R. Gross, H. Christ, and E. Solano, e-print arXiv:cond-mat/0509737.
[11]D. Bozyigit, C. Lang, L. Steffen, J. M. Fink, M. Baur, R. Bianchetti, P. J. Leek, S. Filipp, M. P. da Silva, A. Blais, and A. Wallraff, e-print arXiv:1002.3738v1.
[12]E. P. Menzel, F. Deppe, M. Mariantoni, M. Á. Araque Caballero, A. Baust, T. Niemczyk, E. Hoffmann, A. Marx, E. Solano, and R. Gross, Phys. Rev. Lett. **105**, 100401 (2010).
[13]M. Mariantoni, E. P. Menzel, F. Deppe, M. Á. Araque Caballero, A. Baust, T. Niemczyk, E. Hoffmann, E. Solano, A. Marx, and R. Gross, Phys. Rev. Lett. **105**, 133601 (2010).
[14]A. Zhuravel, A. Sivakov, O. Turutanov, A. Omelyanchouk, S. M. Anlage, A. Lukashenko, A. Ustinov, and D. Abraimov, Fiz. Nizk. Temp. **32**, 775 (2006).
[15]A. P. Zhuravel, S. M. Anlage, and A. V. Ustinov, Appl. Phys. Lett. **88**, 212503 (2006).
[16]The transition from a microstrip hybrid to coplanar waveguides, which are often used in circuit QED, is well studied in literature. Examples are M. C. Maya, A. Lazaro, P. DePaco, and L. Pradell, Microwave Opt. Technol. Lett. **39**, 373 (2003); L. G. Maloratsky, Microwaves RF **3**, 79 (2000).
[17]D. M. Pozar, *Microwave Engineering*, 3rd ed. (Wiley, New York, 2005).
[18]R. E. Collin, *Foundations for Microwave Engineering*, 2nd ed. (Wiley, New Jersey, 2001).
[19]A. D. O'Connell, M. Ansmann, R. C. Bialczak, M. Hofheinz, N. Katz, E. Lucero, C. McKenney, M. Neeley, H. Wang, E. M. Weig, A. N. Cleland, and J. M. Martinis, Appl. Phys. Lett. **92**, 112903 (2008).
[20]D. Koelle and R. Gross, Rep. Prog. Phys. **57**, 651 (1994).